MAGIC-TDAS 08-03
080901 / J. Sitarek

The study of MAGIC I performance for extended sources (2nd draft)

J. Sitarek (MPI)
R. Mirzoyan (MPI)

September 1, 2008

Abstract

A Monte Carlo study about the dependence of MAGIC sensitivity on an extention of a source is presented in this note. Point and extended source responses are compared using both α and θ^2 analyses. We show results of the simulations for both ON-OFF and wobble mode types of observations, and compare them. Additionally the capability of detection of the extension of a source by MAGIC is studied. The analysis is restricted to moderate and high energies (energy threshold 200 GeV).

Contents

1 Simulation and analysis **2**
1.1 MC Sample 2
1.2 Analysis chain 2
1.3 Comparison of wobble and ON MC sample 3

2 α and θ^2 plots **5**

3 Sensitivity reduction for an extended source. **8**
3.1 Quality plots 8
3.2 Dependence of the sensitivity on the source size 10

4 Detection capability for an extention of the source **10**
4.1 MC sample 10
4.2 Description of the method 10
4.3 Two types of errors 12
4.4 χ^2 distributions 13
4.5 Dependence on the observational time and source flux 13

5 Conclusions **15**

6 Work still to be done **15**

1 Simulation and analysis

1.1 MC Sample

For the purpose of this study a dedicated Monte Carlo (MC) sample was generated by using the 6.5 version of Corsika. The MC sample consist of 100 000 gamma-rays with energies 30 GeV – 30 TeV with a spectrum index -1.5. Later in analysis events were re-weighted to obtain desired spectrum index (-2.62 for HEGRA-Crab-like source). Simulations cover the zenith angle range $10° - 30°$. Showers were simulated for all azimuth directions. To increase statistics each of the events was re-used 5 times with a different, random impact point (up to 500m) at the Corsika level.

Corsika events were used to produce four MC reflector samples:

- point source ON events: the source of gamma-rays is located in the camera center
- point source wobble events: the source of gamma-rays is located at the offset of 0.4° from the camera center
- extended source with radius 0.3°, the center of the source is located in the camera center
- extended source with radius 0.3°, the center of the source is located at the offset of 0.4° from the camera center

Extended source is modeled as a flat disc of a radius 0.3°. Inside the disc, the flux from unit area of the disc is constant. There is no flux from radii larger then the radius of the disc. In the case of extended sources, events were three times scattered inside a viewcone of a semiaperture 0.3°. Reflector files were processed with Camera simulation program with total PSF 11.7 mm.

1.2 Analysis chain

MC files were processed with MARS 1-5-4. Camera output files were calibrated with Callisto program and then starified. 6-3 time image cleaning was used in extraction of images.

For a part of the events the $Leakage1$ parameter (a percentage of the size of the image contained in the outermost ring of the camera) has a large value. In this case large part of the shower is outside the camera, the Hillas parameters are wrongly calculated, and the estimation of the energy is more difficult. This effect is more pronounced for higher energies. Also if the image consists of multiple islands, separated from each other, the Hillas parameterization is no longer valid. To improve the quality of the data and to get rid of spark events, a set of cuts is usually aplied in a standard analysis. In order to achieve a compatibility of MC simulations with the used data, several cuts (a "sparks" cut, a maximal leakage cut and a cut in the number of islands) were aplied to the MCs:

- $1.5 - 4. * \log(Conc) < \log(Size)$
- $Leakage1 > 0.2$
- $NumIslands > 3$

The separation of gammas from hadrons was performed by using the Random Forest method. In a general case the hadronness (a likelihood of a given event to be a hadron) can be estimated by using both source dependent and source indepent parameters. The source dependent parameters take advantage of apriori knowledge of the source position in the camera. In the case of an extended source MC sample, we don't know the direction (the position in the camera) of a given photon, we know only the direction of the center of the source. This is why only source independent parameters were chosen for training the hadronness Random Forest. A complete list of used variables is shown below:

- $\log(Size)$
- $2.5 + 5 * \mathrm{floor}(Zd/5)$
- $\log(Size/(Width * Length))$
- $Width$

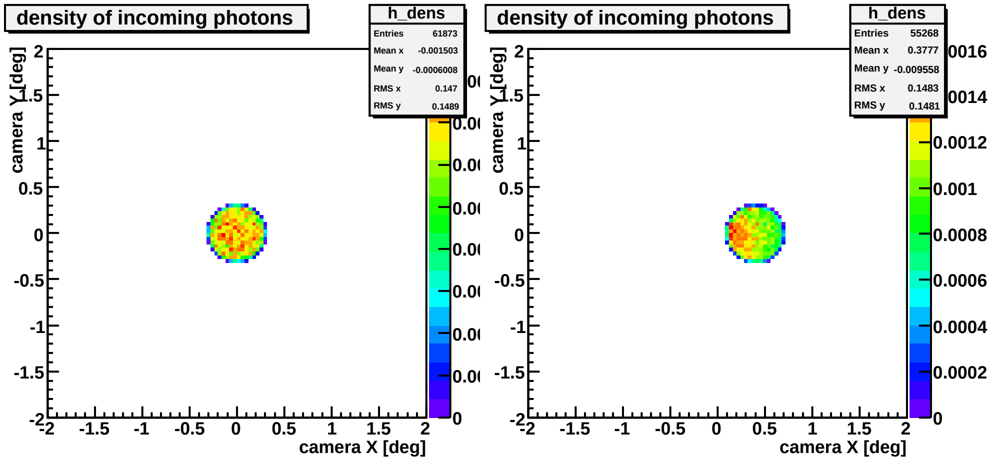

Figure 1: True position in camera coordinates of gamma-rays surviving the cuts. Left: the ON-OFF MC sample (the center of the source is in the center of the camera). Right: the wobble MC sample, with the center of the source placed at the offset 0.4° from the camera center. In both cases the source was simulated with an extension radius 0.3°.

- $Length$
- $Conc$
- $RMSTime$

Both α and θ^2 analyses were done by using the generated MC sample. Hillas parameter α is defined for a point source as an angle between the main axis of the image and a line connecting a centroid of the image with a source position. This definition can also be used in the case of extended source, if we calculate α angle with respect to the center of the source.

In the case of θ^2 the so called DISP method is used. Based on the MC sample a relation between the distance of the centroid of the image to the true source position and elongation of images is established. A calculated value of DISP still gives two possible solutions in opposite sides of the centroid. Choosing of the correct one (ghostbusting) can be done using asymmetry of the image. Then for every event we can estimate a source position. This method seems to be more natural in the case of an extended source. If the error in θ^2 estimation was negligible, then from the θ^2 plot we would get a direct information about the morphology of the extended source.

Training of hadronness and DISP optimization were done with standard MAGIC MC samples with corresponding observation mode (ON or wobble), and off-source data.

1.3 Comparison of wobble and ON MC sample

In the case of an extended source every event is coming from a slightly different direction. After transformation of a coordinate system, each of this directions is corresponding to one point in the camera plane. Then for every extended source event, which survives the cuts, we can project its direction in the camera (fig. 1). The camera acceptance can also be described in terms of two variables ξ and ϕ_{cam}, which are defined as (compare also fig. 2):

- offset ξ: a distance of the event from the center of the source (fig. 3)
- camera angle ϕ_{cam}: an angle between the offset of the event from the center of the extended source and camera X axis (fig. 4). For wobble sample, $\phi_{cam} = 180^\circ$ in the direction of the center of the camera, and $\phi_{cam} = 0^\circ$ in the direction of the outer part of the camera.

The telescope pointing direction can be described by azimuth and zenith angles φ_t and θ_t, and shower pointing by corresponding angles φ_s and θ_s. Then the offset ξ can be calculated from a formula:

$$\cos\xi = \cos(\varphi_t - \varphi_s) * \sin(\theta_t) * \sin(\theta_s) + \cos(\theta_t) * \cos(\theta_s) \tag{1}$$

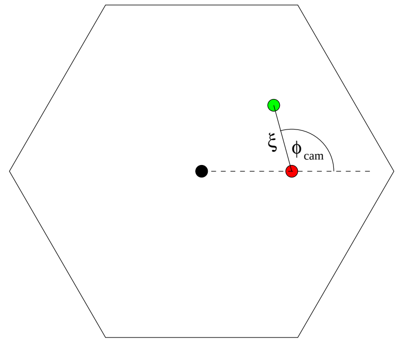

Figure 2: Definitions of the angular distance ξ and the camera angle ϕ_{cam}. Camera and source centers are shown by black and red dots respectively. The true gamma-ray position is marked by a green dot.

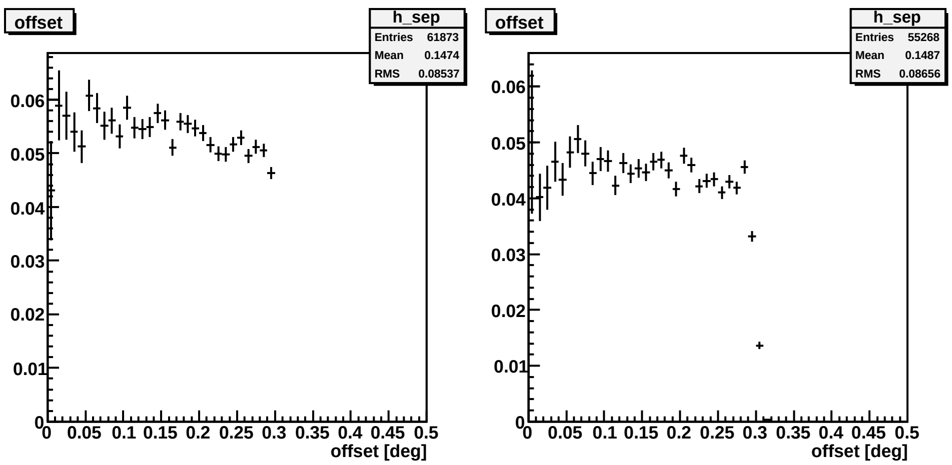

Figure 3: The distribution of ξ, the angular distance between each simulated gamma-ray and the center of the extended source for ON (left figure) and wobble (right) MCs.

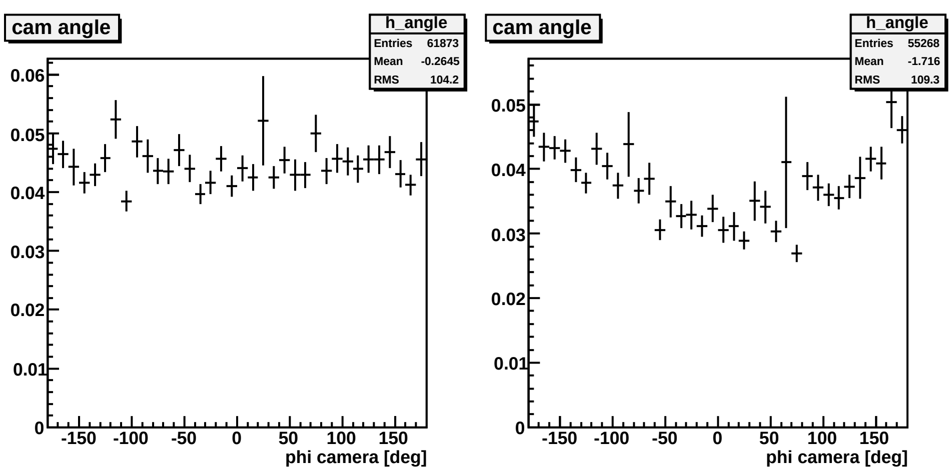

Figure 4: Distribution of the angle in the camera between the offset of the simulated gamma-rays from the center of the extended source and the camera X axis for ON (left figure) and wobble (right) MCs.

In the case of ON MCs, as it would be expected, for a given gamma-ray offset, acceptance doesn't depend on the angle in the camera (a flat distribution in left fig. 4). A slow decrease of the collection area with the distance from the camera center is clearly seen in a left part of fig. 3. It is due to the finite size of the trigger area of the MAGIC camera.

On the other hand for the wobble MCs there is a clear anisotropy with more events from the direction of the center of the camera (right fig. 1). Also the distribution of the angular distance ξ is slightly less steep for the wobble case that for ON (compare left and right fig. 3).

The collection area in the case of wobble mode is smaller than in the case of ON observations. Nevertheless the difference is rather small: only $\sim$ 20% decrease in the collection area of the wobble mode observations with respect to ON). This result is more optimistic than the result of MAGIC-TDAS 07-01 in which the drop in the gamma efficiency at the wobble position 0.4° was expected to be around 50%. One of possible reasons for this discrepancy could be that in this work the hadronness Random Forest and the DISP optimization used for ON and wobble sample were trained on wobble and ON MCs respectively, while in TDAS 07-01 no optimization for the source offset was performed.

This decrease of sensitivity in wobble mode observations is compensated by the fact that the on-source and the off-source data are taken simultaneously, so the time which can be spend on ON observations is increased. Moreover, in the case of wobble mode observation multiple OFF-positions can be chosen. This increases the background statistics.

2 α and θ^2 plots

Gamma-rays from a source can be detected as an excess of signal events at low values of α or θ^2 over the background. In the case of extended sources there is a natural broadening of those distributions, which increase the background, and decrease the sensitivity. To check how big is the effect we first compare α and θ^2 plots for sources with different extension radii r_{ext} with corresponding plots for a point source. Sample MC α and θ^2 distributions for both point and extended sources of radius r_{ext} are presented on the upper part of fig. 5. All distributions are normalized to the rate from HEGRA-Crab-like source with spectrum index -2.62. A cut in size (> 200phe) and in hadronness (< 0.15) are applied. For considered zenith range ($10 - 30°$), the cut in size is corresponding to threshold energy $\sim$ 200 GeV.

In the case of an extended source a broadening of both distributions is clearly visible. For θ^2 a characteristic broadening scale is equal to $\theta_b^2 \approx r_{ext}^2 + \theta_{PSF}^2$, where $\theta_{PSF} = 0.1°$ is the MAGIC point spread function for gamma-rays from a point source. A corresponding characteristic α_b value can be estimated as: $\alpha_b \approx \arctan(\sqrt{r_{ext}^2 + \theta_{PSF}^2}/1.2°)$ In the case of $r_{ext} = 0.3°$, $\theta_b^2 \approx 0.1°^2$, $\alpha_b \approx 15.°$.

θ^2 and α distributions look different for a very extended source. The signal peak is much more pronounced in the case of θ^2 than in α. Since θ^2 is the squared distance between the source center and the reconstructed source position, it can be just broadened by source extension squared. On the other hand in the case of α, if individual source position is off-center in one direction, and the image itself is on the other direction, α values calculated with respect to the center of extended source can be quite big. Then peak in α distribution becomes flat at low α angles.

Using cumulative distributions we can calculate a value of the cut in α or θ^2 for a given gamma-ray efficiency. Results of this calculation are shown in fig. 6.

Compared to the point source, there is no visible change in the cut efficiency up to a source radius 0.05°. For a disc of radius 0.1° the cut value is slightly increased (by about 20-30%). For a source extension $\sim 0.3°$ the cut in α has to be increased even 3 times, while in θ^2 only about 2 times compared to a point source.

In the case if it is desired to have a high gamma efficiency ($\gamma_{eff} = 0.8$), the θ^2 analysis is not so optimal, because of the very loose cuts. [1].

[1] Ghostbusting method in $\sim$ 15% cases fails to choose a correct direction of the source, producing large (> 0.5 deg^2) values of θ^2. So if requested gamma-ray efficiency is high ($\sim$ 80%) almost all gamma-rays with correctly estimated direction of the DISP have to be included in the cut, which results in very loose cuts.

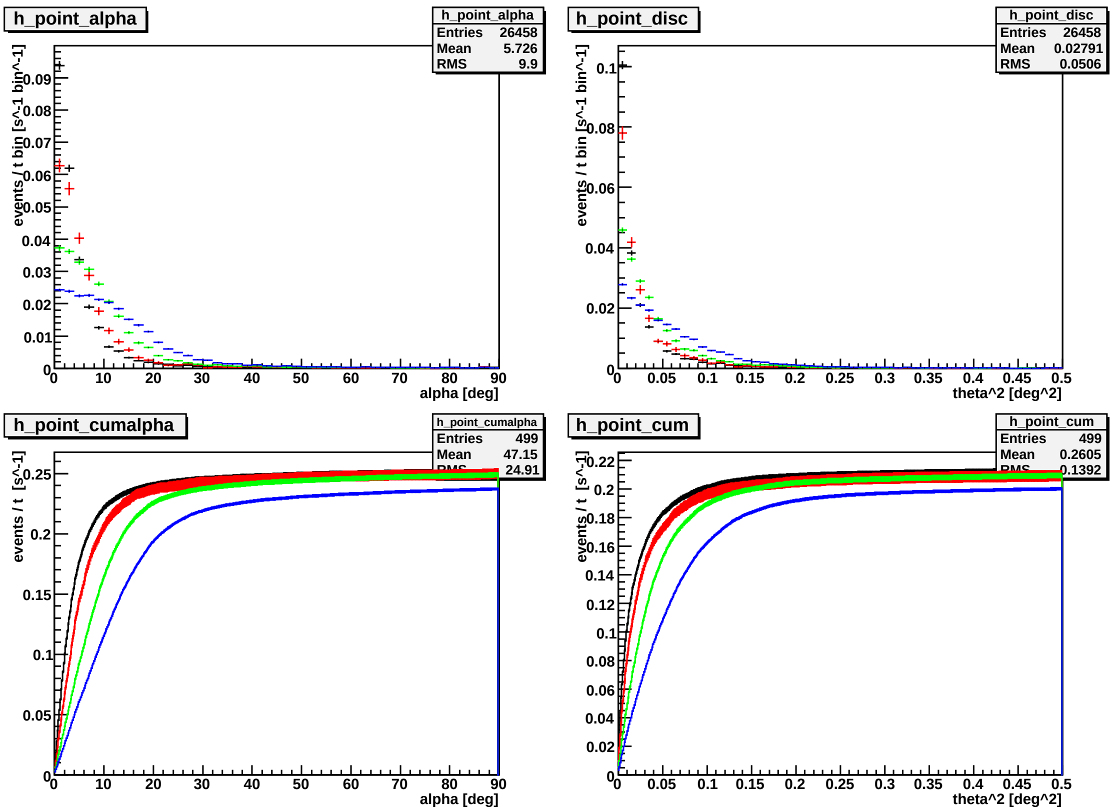

Figure 5: Upper plots: α (left figures) and θ^2 (right) plots for MC gammas. Size cut > 200 phe, hadronness cut < 0.15. Lower plots: corresponding cumulative distributions. Different colors stand for different source sizes: point source (black), disc radius $r_{ext} = 0.1°$ (red), $0.2°$ (green), $0.3°$ (blue).

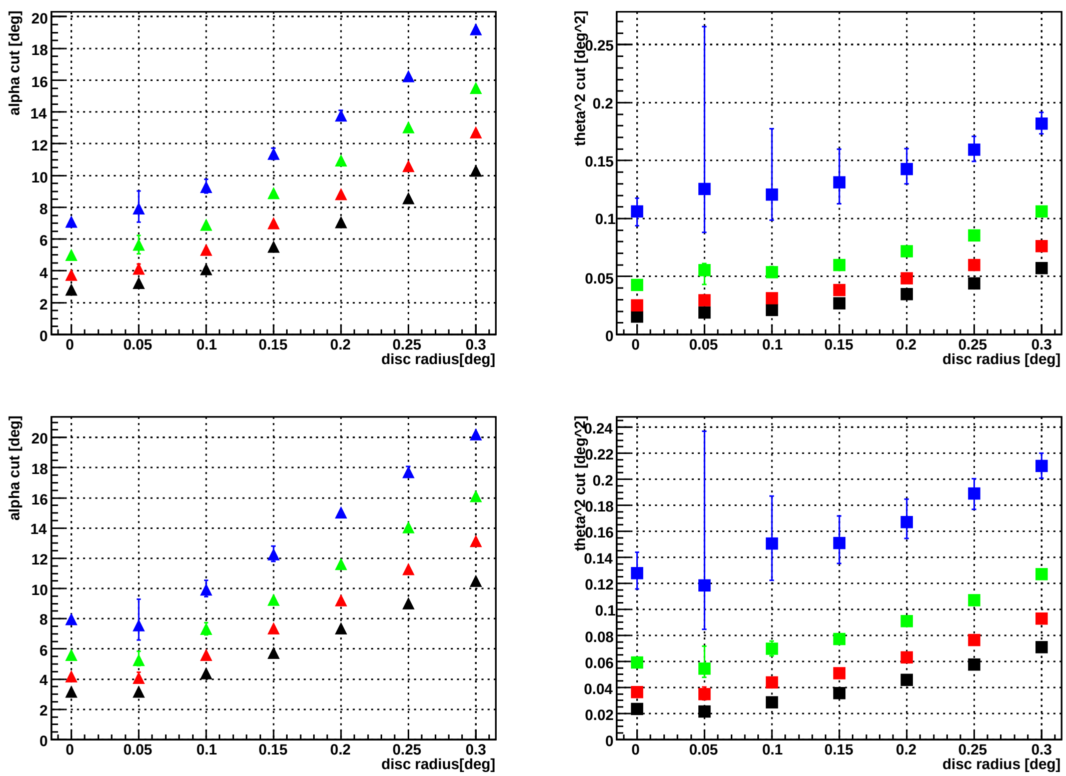

Figure 6: Values of α (left figures) and θ^2 (right) cuts as a function of radius of the extended source. Different colors stand for different α or θ^2 cut efficiencies: 0.5 (black), 0.6 (red), 0.7 (green), 0.8 (blue). Upper figures for ON MCs, and lower pictures for wobble MCs. Point source values are plotted as disc radius = 0.

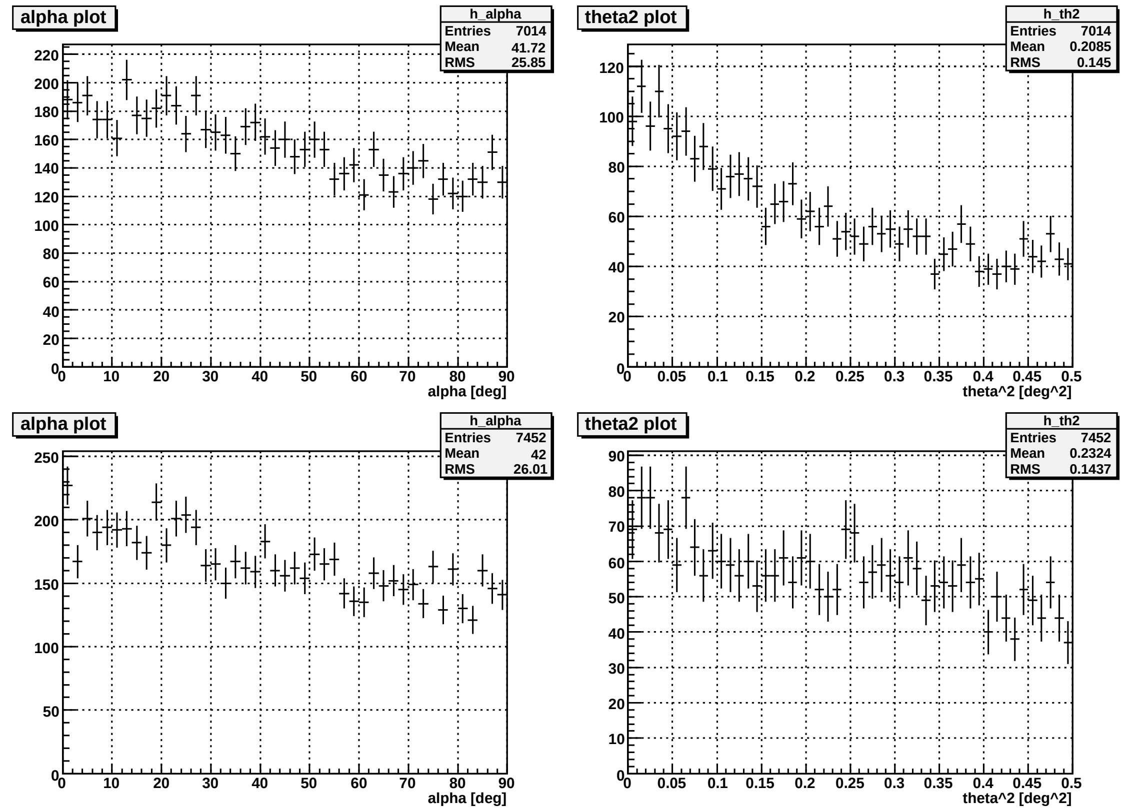

Figure 7: Distributions of α (left figures) and θ^2 (right) for the OFF data. Upper figures for the ON MCs, and lower for the wobble MCs.

3 Sensitivity reduction for an extended source.

3.1 Quality plots

A good quantity to compare a telescope's performance for an extended source with that of a point source is the quality factor defined as:

$$Q = \frac{\gamma_{eff}}{\sqrt{h_{eff}}}, \tag{2}$$

where γ_{eff}, h_{eff} are respectively gamma-ray and background efficiencies of α or θ^2 cut. The gamma ray efficiency was calculated directly from the produced MCs. In principle the hadron efficiency could be also estimated from a dedicated MC sample. Unfortunatly simulations of hadronic showers are much more CPU time consuming and less robust than for purely electromagnetic showers. On the other hand hadronic showers can be obtained directly from the data. Estimation of α and θ^2 cut efficiencies for background hadrons were obtained using a small sample ($\sim$ 1h) of the OFF data of a similar zenith angle distribution as the MCs.

Source depended parameters for this sample were recalculated two times, to obtain both wobble and ON/OFF mode. Background α and θ^2 distributions are shown in fig. 7. Because of the finite size of the trigger region in the MAGIC camera, α and θ^2 plots look different for the background in the case of wobble and ON-OFF observations.

The quality factors are ploted in fig. 8. As in the case of calculated values of the efficiency of cuts, up to the source radius 0.05° there is no significant drop in the quality factor and one can observe only a small one for a source with a radius 0.1°. For source extention radius 0.3° the decrease in the quality factor is already significant: $\sim$ 40%. The quality factor only weakly depends on the efficiency cut in the range 0.5-0.7. In the case of θ^2 cut with an efficiency 0.8, the quality factor is much lower, because of above-mentioned misclassified DISP events. On average θ^2 analysis provides $\sim$ 20% higher quality factors than the α analysis. The presented here analysis is commited to extended source studies, no source dependent parameters were used in training of the Random Forest.

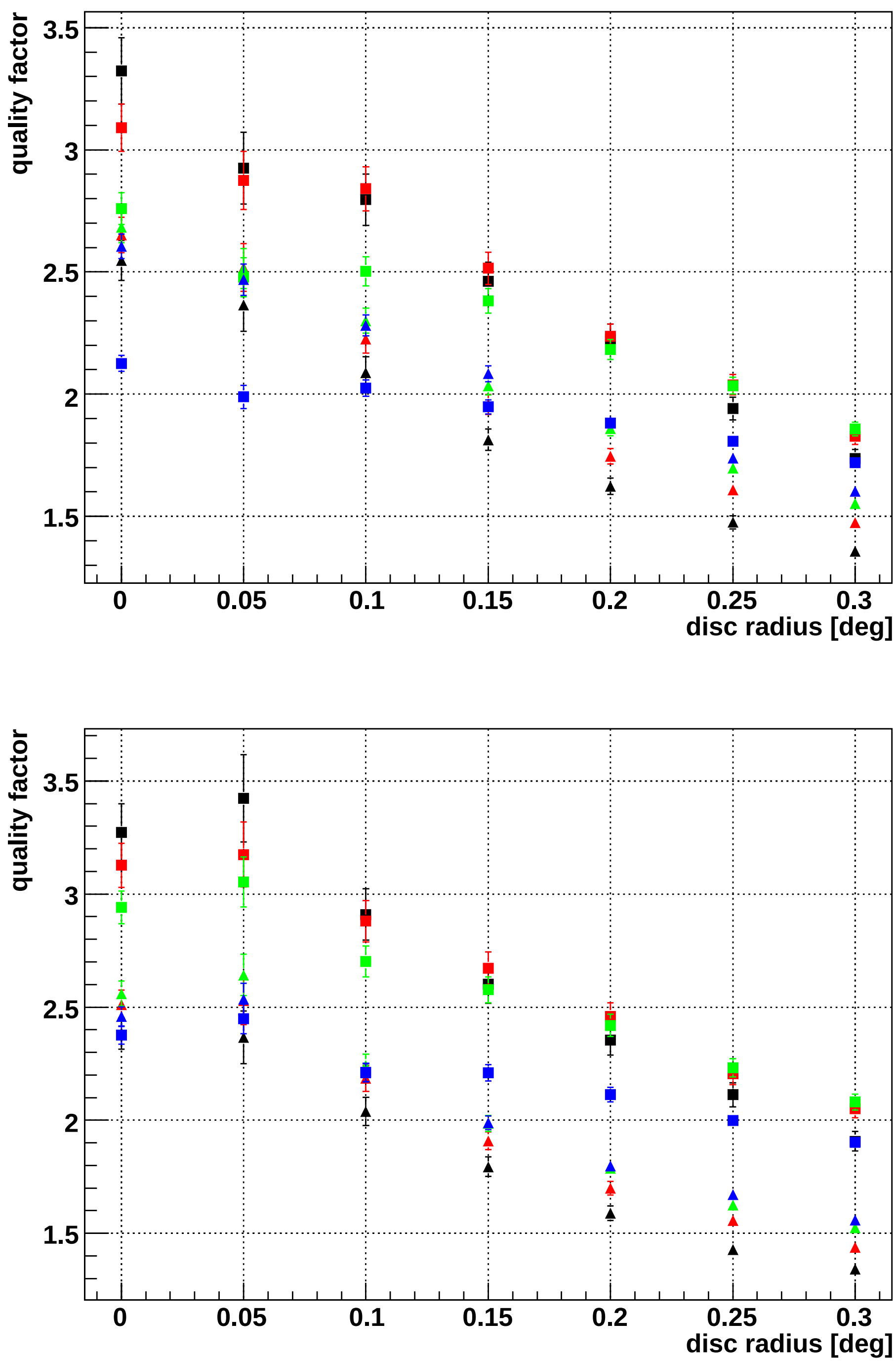

Figure 8: Dependence of the quality factor on the extension of the source size. Different colors stand for different α (triangles) or θ^2 (squares) cut efficiencies: 0.5 (black), 0.6 (red), 0.7 (green), 0.8 (blue). Upper figure for ON MCs, and lower figure for wobble MCs.

source radius	ON-OFF observations θ^2	ON-OFF observations α	Wobble observations θ^2	Wobble observations α
point	16	15	14	12.5
0.1°	15	13.5	13	11
0.2°	13	11.5	11.5	9
0.3°	11	9.5	10	7.5

Table 1: Values of the significance (in sigmas) for different radii of a source extension. The observation time is equal to 1h ON and 1h OFF (for ON-OFF mode) or 1h of simultaneous ON and OFF (in the case of wobble)

3.2 Dependence of the sensitivity on the source size

The quality factor as defined in eq. 2 cannot be used for comparing directly the wobble and the ON-OFF observarions, because it doesn't take into account that the colection area in the case of wobble observations is smaller than in the case of ON-OFF observations. One can do this comparison by calculating the significance obtained from 1h of observations of a Crab-like imaginary source.

Assuming a given α or θ^2 cut (calculated for a fixed gamma efficiency) a number of expected excess events in the given time can be calculated from the MC files. Using the information on the remaining background events after given cuts one can calculate the significance according to the Li & Ma formula. Results of this calculation are shown in fig. 9 (the dip for source radius 0.05° is only caused by the lack of statistics) and are summarized in table 1. In both cases the ratio of the OFF data to the ON data was set to be one.

Estimated from the MCs, the sensitivity for one hour of Crab-like point source observations in a ON-OFF mode is up to $16\sigma/\sqrt{\mathrm{h}}$ in the case of θ^2 analysis. In wobble mode observations this significence is decreased to $14\sigma/\sqrt{\mathrm{h}}$. Calculated sensitivity for ON-OFF mode assume that except of the ON data, the same amount of the OFF source data is already available. If the observational time have to be split between ON and OFF observations, then the value of the sensitivity for ON-OFF observations, observed equal time, should be decreased by a factor of $\sqrt{2}$. Moreover in the wobble analysis we used only one OFF position. Using additional OFF positions will increase background statistics, which will increase the significance in the wobble mode observations. Those values are obtained using size cut > 200 phe, which in this analysis corresponds to energy threshold ~ 200 GeV. At very low energies (< 100 GeV) differences between wobble and ON-OFF observations might be more complex.

The α analysis gives $10-20\%$ lower values of the significance then the θ^2 analysis. Dependence of the significance on the source extension is more or less the same for both analysis types and observation modes. Up to the source extension radius of the order of $r_{ext} = 0.1°$ significance drops slowly (only $\sim 10\%$). For $0.1° < r_{ext} < 0.3°$ the slope of the dependence is steeper. For $r_{ext} = 0.3°$, the significance is reduced only by $\sim 40\%$.

4 Detection capability for an extention of the source

4.1 MC sample

The MC sample used in this section is slightly different than the one described in 1.1:

- a total number of generated showers is two times more,
- only a wobble mode is considered (both point and extented sources),
- a simulated value of the mirror PSF is slightly lower: 10.6mm.

4.2 Description of the method

Let's consider two α (or θ^2) distributions: one for a point source, and an another one for a source with a not known extension. In order to check if the second distribution is also consistent with a point source, we can do a χ^2-test. The test should be done not for the full histogram, but only for the bins in which one can find a signal. Extending the test to the full histogram doesn't bring any new information, and in contrary, it is increasing statistical fluctuations which decrease the distinguishing power of the test.

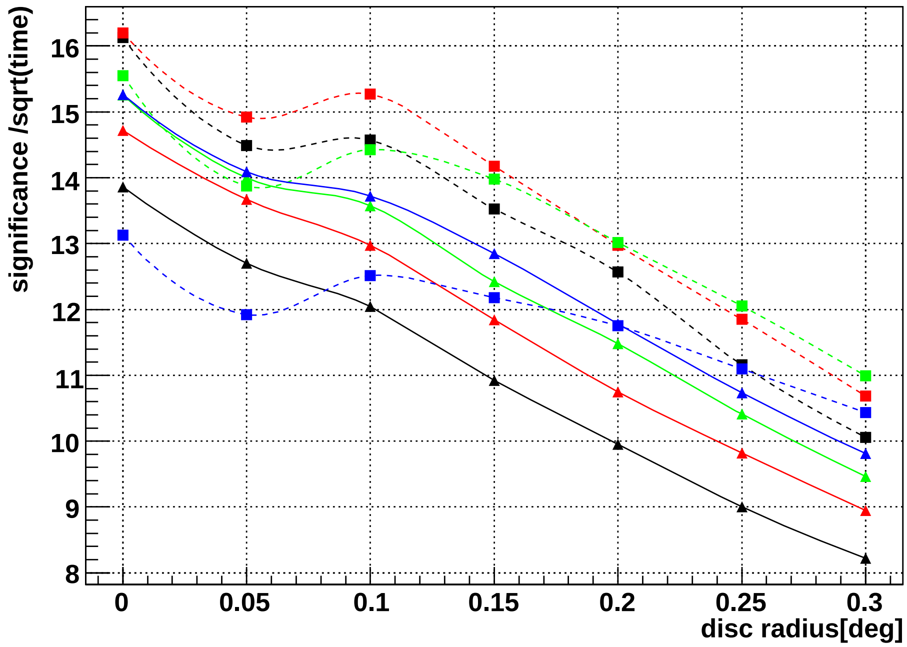

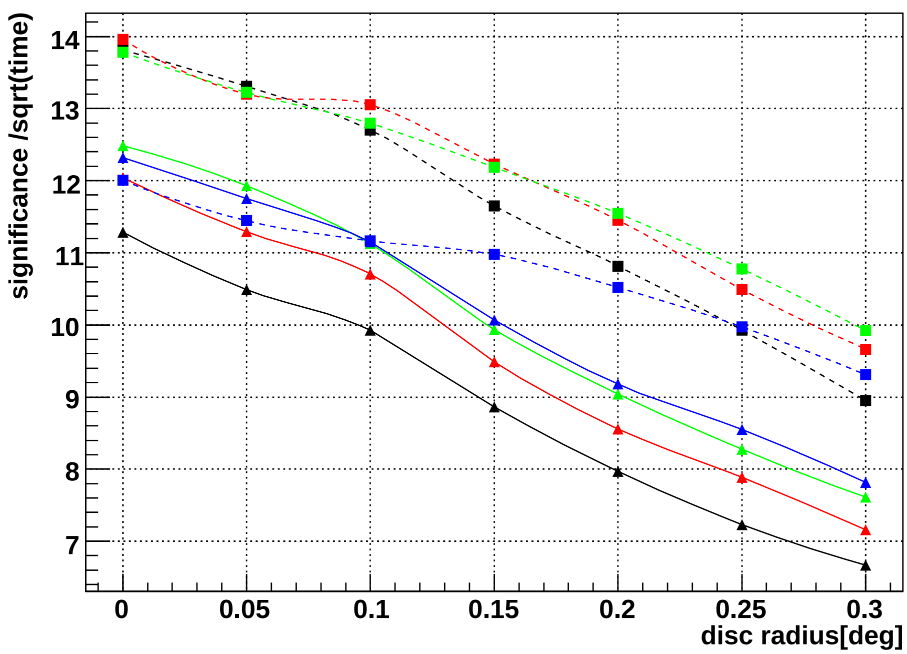

Figure 9: The significance (in sigmas per square root of hour of the source observations) as a function of an extention of the source. Different colors stand for different α (solid lines) or θ^2 (dashed) cut efficiencies: 0.5 (black), 0.6 (red), 0.7 (green), 0.8 (blue). Hadronness cut < 0.15, size cut > 200 phe. Upper figure for the ON position, and lower figure for the wobble position.

Let's now ask a question: what minimum source size can be detected by MAGIC ? The answer is obviously dependent on the observation time and on the flux from the source.

Another important parameter is the spectrum index of the source. For a flat spectrum there are many high energy events, for which determination of the Hillas parameters is more precise, and resulting α and θ^2 distributions are narrower. In this case it is easy to find extension of the source. Also PSF of the mirrors of the telescope has an effect on the natural broadening of the α and θ^2 distributions.

Let's consider now two MC samples: one for a point source, and a second one for a source with a given extension radius r_{ext}. Both samples are weighted by a HEGRA-Crab-like spectrum with an index -2.62. We can assume an observation time of t hours. Then with a proper normalization one can obtain the expected α and θ^2 distributions.

Since we are dealing with weighted histograms, we should use a χ^2 formula as presented in [3]:

$$\chi^2 = \sum_{i=1}^{r} \frac{(W_1 w_{2i} - W_2 w_{1i})^2}{W_1^2 s_{2i}^2 + W_2^2 s_{1i}^2}, \tag{3}$$

where w_{1i}, w_{2i} stand for weights of the first and the second histogram in the bin number i and s_{1i}, s_{2i} are the estimated errors of those weights. $W_j = \sum_{i=1}^{r} w_{ji}$ are sums of weights. If both distributions are the same then χ^2 follows a χ^2_{r-1} distribution.

The calculated value of χ^2 can be represented also as a probability p that differences between two compared histograms are only because of statistical fluctuations:

$$p = \int_{X^2}^{\infty} \chi^2_{r-1}(x)dx. \tag{4}$$

On the other hand the value of a probability can be transformed into more intuitive "significance" S in the units of sigma, which is defined by the relation:

$$p = \int_{S}^{\infty} \mathcal{N}(0,1)(x)dx, \tag{5}$$

where $\mathcal{N}(0,1)$ is a gaussian distribution with a mean 0 and a standard deviation 1.

4.3 Two types of errors

What should be keeped in mind is that we have now two sets of errors associated with our MC sample. The distributions of gammas in the real data should fluctuate around the predicted α and θ^2 distributions with a poissonian error (in every bin the error is the square root of the content of this bin). Moreover since the γ-ray signal in the real data is extracted from a background, this error should be appropriately enlarged. If in a given bin the expected number of gammas is equal to N_g, and the expected background is equal to N_b, then the total error of the extracted gamma distribution can be calculated as:

$$\Delta N_g = \sqrt{N_g + 2N_b} \tag{6}$$

This error will be used in the χ^2 test as a measure of statistical fluctuations which deteriorate the power of finding if the source has an extension.

On the other hand since only a finite amount of MC showers is used for calculation of the expected α and θ^2 distributions, there is a statistical error on the estimation of those distributions. Let's call it a "MC error". This error is only a measure how precise are the simulations. If "MC error" is larger than the predicted poissonian error it means that the differences between point and extended source MCs can be a result of statistical fluctuations of the MC sample rather than the intrinsic difference between those two distributions.

On fig. 10 both types of errors are compared for the case of 1h observations of a source with a Crab spectrum.

Now let's consider how those errors change if we increase the observation time. Since the estimated gamma excess will increase linearly with time, the estimated relative poissonian error will decrease as a square root of time. On the other hand, the α or θ^2 distribution is still estimated from a full MC sample, and the dependence on time is done with simple scaling. It means that the relative "MC error" remains the same. We perform our calculations as long as the "MC error" is less than 50% of the poissonian error. For higher values of the observation time produced MC sample is not enough for drawing conclusions.

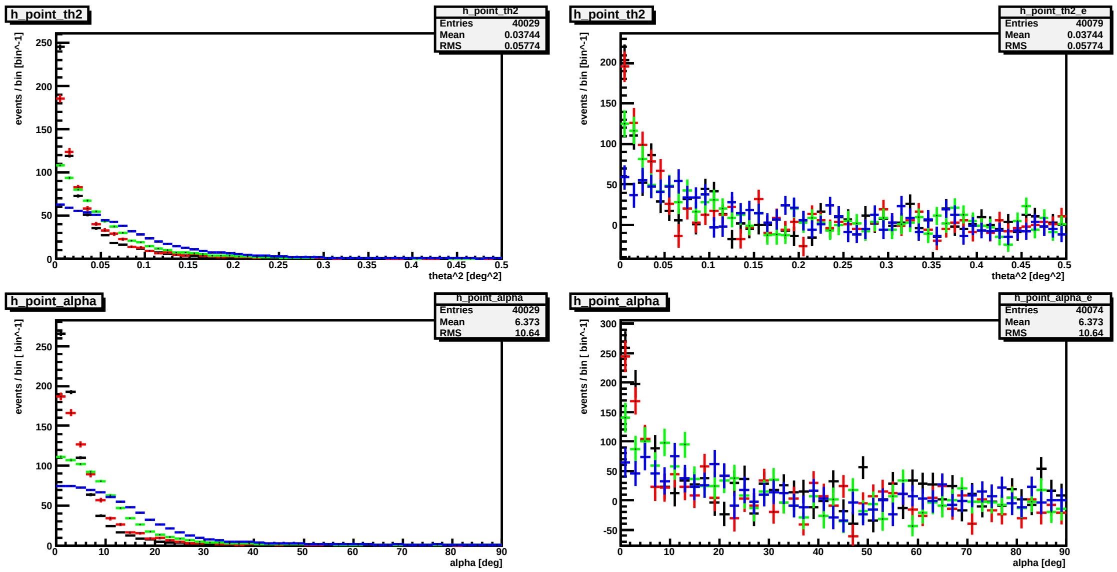

Figure 10: Expected θ^2 (upper figures) and α plots (lower figures) for MC gammas. Different colors stand for a different source extensions: a point source (black), a disc of a radius $r_{ext} = 0.1°$ (red), $0.2°$ (green), $0.3°$ (blue). In left figures vertical error bars show a statistical uncertainty of the MC sample. In right figures those errors represent real poissonian errors calculated according to (6). Observational time 1h, hadronness cut < 0.15, size cut > 200 phe.

source radius	α analysis					θ^2 analysis				
	$\langle\chi^2\rangle$	n_{dof}	$\langle\chi^2\rangle/n_{dof}$	$p(\langle\chi^2\rangle)$	S	$\langle\chi^2\rangle$	n_{dof}	$\langle\chi^2\rangle/n_{dof}$	$p(\langle\chi^2\rangle)$	S
$0.1°$	6.8	3	2.3	$8 \cdot 10^{-2}$	1.4σ	10.9	6	1.8	$9 \cdot 10^{-2}$	1.3σ
$0.2°$	24.	5	4.8	$2 \cdot 10^{-4}$	3.5σ	37.	9	4.1	$2 \cdot 10^{-5}$	4.1σ
$0.3°$	40.	8	5.0	$3 \cdot 10^{-6}$	4.5σ	68.	12	5.7	$9 \cdot 10^{-10}$	$6.\ \sigma$

Table 2: The mean χ^2, a number of degrees of freedom, the fluctuation probability and the significance of a source extension. for different radii of a source. 1h of a wobble mode observation. a 70% gamma efficiency cut, a hadronness cut < 0.15 and a size cut > 200 phe.

4.4 χ^2 distributions

To check capability of MAGIC to detect the extension of a source we compare a point source α (or θ^2) MC distribution with a similar distribution for a disc source with a given radius r_{ext}. After scaling the distribution to a given observational time we calculate errors according to eq. 6 in every bin, and then we scatter the value with this error. Both histograms are then compared using the χ^2 value defined by eq. 3. Only bins fulfilling a gamma efficiency cut are used for comparison of both histograms. The entire procedure is repeated 10^4 times.

Sample distributions of χ^2, obtained in the case of observing a source with a Crab-like spectrum for 1h, are shown in fig. 11. The corresponding fluctuation probability $p(\chi^2)$ distributions are shown in fig. 12.

From a distribution of χ^2 we obtain a mean value $\langle\chi^2\rangle$, and the corresponding probability $p(\langle\chi^2\rangle)$ according to eq. 4. The probability is converted into a significance using eq. 5. Values obtained from distributions shown in fig. 11 are presented in table 2.

4.5 Dependence on the observational time and source flux

On fig. 13 a significance of the extension of the source is shown as a function of time for flux of a source equal to 0.25, 1 and 4 Crab Units. Let's consider a source with a Crab-like flux and an extension radius $r_{ext} = 0.3°$. After 70 min of the observation time a 5σ discrepancy between the source α plot and an α plot for a point source can be seen. If the θ^2 analysis is used this time is decreased to only 45 min. For a much smaller source extension ($r_{ext} \sim 0.1°$) both methods seem to give similar results: 5σ obtained in $\sim$ 5-6 h. Necessary observational times for a 1 C.U. source are summarized in table 3.

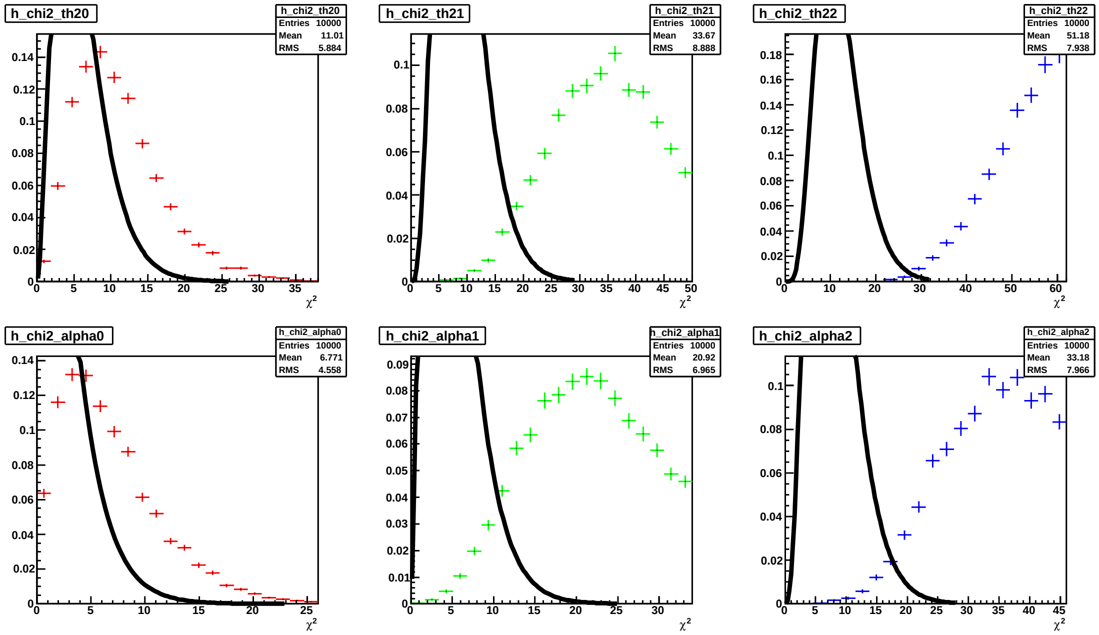

Figure 11: The χ^2 distribution of a comparison of a point source with an extended one. Upper figures are obtained with a θ^2, lower with a α analysis. Different colors stand for different radii of an extended source: $r_{ext} = 0.1°$ (red), $0.2°$ (green), $0.3°$ (blue). A thick black curve in every figure is the χ^2 distribution in the case if both compared histograms are from the same distribution. The observational time 1h, hadronness < 0.15, size > 200 phe.

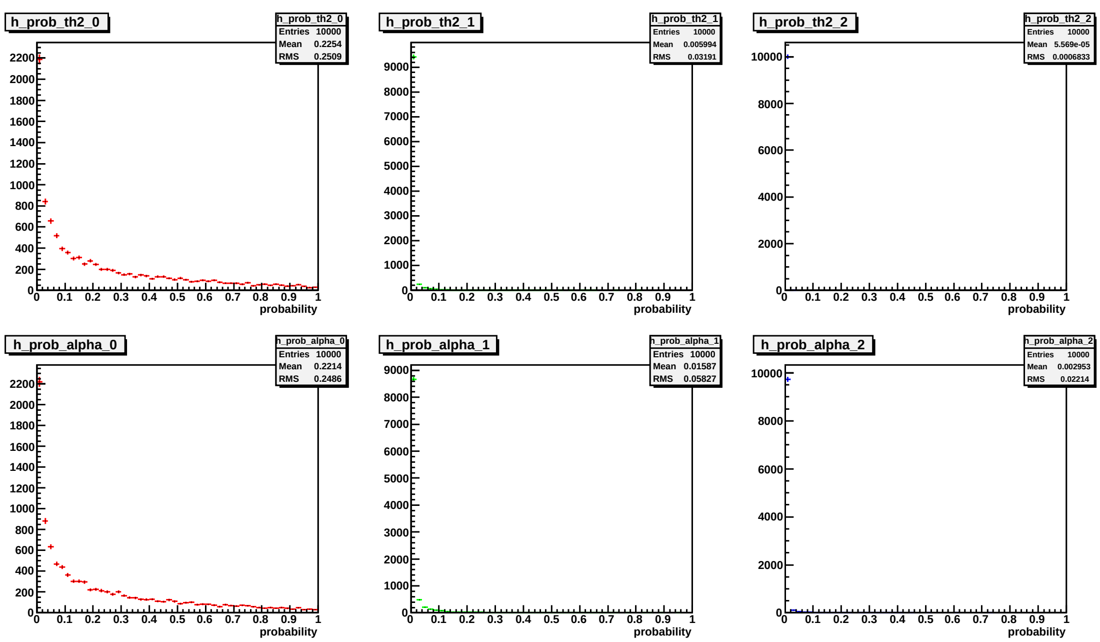

Figure 12: As in fig. 11, but the distribution of the probability that differences between two histograms are only because of statistical fluctuations (calculated according to eq. 4)

r_{ext}	θ^2 analysis	α analysis
$0.1°$	7*	8
$0.2°$	1.4	1.8
$0.3°$	0.8	1.2

Table 3: The observational time (in hours) needed for claiming an extension of a source with a 5 σ confidence level. Both α and θ^2 analyses are considered. r_{ext} stands for the radius of the source. Values marked with a star are obtained using an extrapolation and therefore can have a large systematic error.

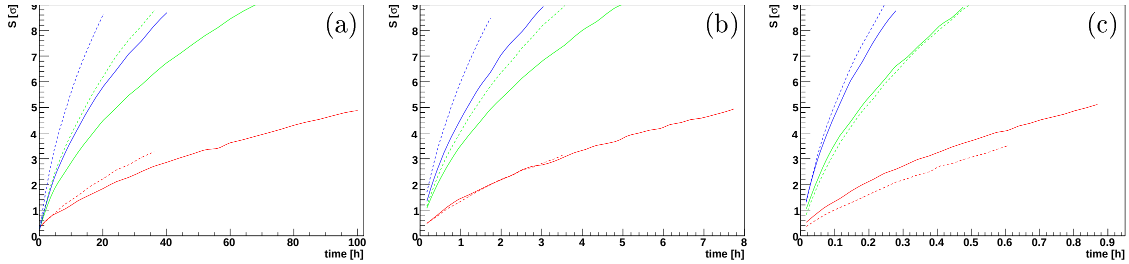

Figure 13: The increase of the significance (in the units of sigma) of the source extension with the observation time in the wobble mode. Different colors stand for different radii of an extended source: $r_{ext} = 0.1°$ (red), $0.2°$ (green), $0.3°$ (blue). Total flux from the source is equal to 0.25 C.U. in figure (a), 1 C.U. in (b) and 4 C.U. in (c). Results from the α analysis are ploted with solid lines, and from the θ^2 analysis with dashed lines.

For a source with a lower flux the needed observation time is greatly increased (compare fig. 13 (a) and (b)). A $r_{ext} = 0.3°$ extension of a source can be discovered after 16h or 9h in the case of α and θ^2 analysis respectively. If predicted source extension is of the order of a MAGIC PSF ($0.1°$), it can be distinguished from a point source after $\sim 70 - 100$ h of observations.

5 Conclusions

- Reduction of the sensitivity for an extended source:
  - If a given source has an extension of $r_{ext} \sim 0.1°$, for obtaining the same gamma efficiency as in the case of a point source, one should cut the angular parameters by $\sim 20 - 30\%$ looser. This results in only modest ($\sim 10 - 15\%$) loss in sensitivity.
  - Even in the case of a significantly extended source ($r_{ext} = 0.3°$) the loss in the sensitivity is only about 40%.
- Comparison of the wobble mode with the ON-OFF mode:
  - Comparing with the ON-OFF mode, the reduction of the sensitivity in the case of the wobble mode observation is only $\sim 20\%$. The value is consistent with the value quoted in [2] ($\sim 15\%$ for pre-MUX data). This result is still valid even in the case of an extended source with a radius $0.3°$.
  - The drop in the sensitivity is smaller than the gain because of taking OFF data simultaneously. This is why, even in the case of a slightly extended source (an extension radius $\lesssim 0.2°$) the wobble mode observations seems to be a better option than the ON-OFF observations. For bigger extentions of the source leakage of the signal into the background region can become a problem.
- Source independent α and θ^2 analysis:
  - In presented here type of analysis (the Random Forest was trained with no source depended parameters) a θ^2 cut is more powerful that an α cut both for a point-like and extended sources. The difference in the sensitivity is of the order of 20%.
- Detection of source extension
  - For a homogeneous disc source with a Crab-like spectrum, an extension radius of the order of $r_{ext} \sim 0.3°$ can be detected after 45min.
  - In the case of a very extended source the α analysis needs up to 50% more observation time than the θ^2 analysis. For a small extension both methods give similar results.

6 Work still to be done

A few secondary effects are still not covered in this TDAS note and will be addressed in the near future.

- The extraction of an extended signal in a presence of a point source. This situation occurs for example in a case of a theoretical AGN halo [2].
- How much a performance of the MAGIC telescope for extended sources is dependent on the telescope PSF.
- Dependence of the α and θ^2 plots on the source spectrum index.
- Extended sources with a different profiles than a flat disc.

References

[1] MAGIC-TDAS 07-01

[2] MAGIC-TDAS 07-03

[3] Gagunashvili N.D., Comparison of weighted and unweighted histograms, (2006), arXiv:physics/0605123v1

[2] Primary gamma rays coming from a source are absorbed in a pair production process. Those pairs then scatter the CMB radiation producing a second generation of gamma-rays, but since leptons could be deflected in a magnetic field, secondary gamma rays will come from a different direction than the primary gamma rays, producing a halo around the point source.